State Estimation with Consideration of PMU Phase Mismatch for Smart Grids

Peng Yang[1], Zhao Tan[1], Ami Wiesel[2], and Arye Nehorai[1]

[1]Preston M. Green Department of Electrical & Systems Engineering Washington University in St. Louis, MO 63130
[2]School of Computer Science and Engineering, The Hebrew University of Jerusalem, Jerusalem 91904, Israel

***Abstract*—Phasor measurement units (PMUs) are time synchronized sensors for power system state estimation. Despite their promising advantages, large scale deployment of PMUs is still limited. One of the reasons is the high cost of their exact synchronization. In this paper, we consider the use of cheaper and less accurately synchronized PMUs, but compensate for these imperfections via signal processing methods. We introduce a statistical model for power state estimation using these impaired units. We then derive an alternating minimization technique and a parallel Kalman filter for static and dynamic estimation, respectively. Numerical examples demonstrate the improvement in estimation accuracy of our algorithm compared with traditional algorithms when phase mismatch is present. Our results suggest that the phase mismatches can be largely compensated as long as there is a sufficient number of PMUs and the delays are small.**

I. Introduction

In recent years, phasor measurement units (PMUs) [1] have become increasingly important in power system state estimation [2]-[4]. The traditional supervisory control and data acquisition (SCADA) system has a low sample rate and uses a complex nonlinear model for state estimation, and the measurements are not synchronized. Modern PMUs provide synchronized phasor measurement and linear state estimation. Their sampling rate is much higher, enabling real-time estimation of the power system's state and a fast response to abnormalities.

Ideally, PMUs use a costly global positioning system (GPS) radio clock as a common time source. This impedes large scale installation of PMUs and limits their use in practice. Indeed, recent works consider the optimal placement of PMUs to permit the installation of a minimum number of PMUs [5]-[7]. However, without enough PMUs, their advantage in linear measurements cannot be fully exploited, and traditional low sample rate nonlinear measurements still have to be used for full system state estimation.

Large scale deployment of PMUs inevitably result in the use of PMUs from multiple vendors. However, due to different standards, protocols, and designs, the synchronization of PMUs from different vendors is a problem. According to [8], the clocks of PMUs need to be accurate to 500 nanoseconds to provide the one microsecond time standard needed by each device performing synchrophasor measurement. However, a test shows that PMUs from multiple vendors can yield time dissynchronization of about 47 microseconds [9]. In addition, to reduce the cost of PMUs for large scale deployment, low cost PMUs with imperfect synchronization may be used. These PMUs may use alternative synchronization mechanisms, e.g., the Precision Time Protocol (PTP) as defined in IEEE-1588 standard [10]-[12], or the radio station WWVB [13]. According to the IEEE-1588 standard, instead of purely using a GPS radio clock for each of the devices, only the "masters" are equipped with global clocks. The "slaves" use local clocks, and a sync message is transmitted from a "master" to its "slaves" every few seconds. Alternatively, the WWVB radio station uses a pulse amplitude modulated signal with a bit rate of 1b/s to synchronize widely separated clocks, with lower accuracy compared with GPS radio clocks. As a general model, in this paper we consider different PMUs are synchronized every $T_{\rm sync}$ seconds, and use imperfect local clocks between consecutive synchronizations.

The traditional measurement model assumes accurate synchronization or models the imperfections as additive noise[14]-[17]. In this paper, we build a new model for state estimation which takes into account the PMU phase mismatches. Then we propose static and dynamic estimation algorithms based on alternating minimization (AM) and parallel Kalman filtering (PKF) [18], respectively. Numerical examples demonstrate that our proposed algorithm provides more accurate state estimates when the PMUs are imperfectly synchronized. Our results suggest that the phase mismatches can be largely compensated as long as there is a sufficient number of PMUs and the delays are small.

We organize the rest of this paper as follows. In Sec. II we describe the system model considering phase mismatch. In Sec. III we introduce the proposed algorithms for state estimation with phase mismatch. We show numerical examples in Sec. IV, and conclude the paper in Sec. V.

Notations: We use $\{\cdot\}^{\rm r}$ to denote the real part, $\{\cdot\}^{\rm i}$ to denote the imaginary part, and superscript T to denote vector transpose.

II. System Model

We consider a grid model with P buses connected via branches. The continuous (denoted with superscript $\rm c$) voltage signal on bus p at time instance t is defined as

$$\overline{E}_p^{\rm c}(t) = E_p^{\rm c}(t)\cos\left(2\pi f_{\rm c} t + \varphi_p^{\rm c}(t)\right) \tag{1}$$

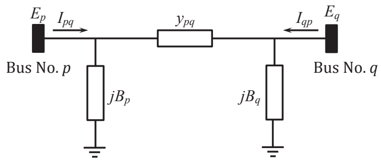

Fig. 1: Bus branch model.

where f_c is the power frequency. The phasor representation of $\overline{E}_p^{\mathrm{c}}(t)$ is $E_p^{\mathrm{c}}(t)e^{j\varphi_p^{\mathrm{c}}(t)}$, with $E_p^{\mathrm{c}}(t)$ denoting the magnitude and $\varphi_p^{\mathrm{c}}(t)$ denoting the phase. For simplicity, we work with discrete phasor time series

$$\begin{aligned} E_{p,k} &= E_p^{\mathrm{c}}(kT), \\ \varphi_{p,k} &= \varphi_p^{\mathrm{c}}(kT), \end{aligned} \tag{2}$$

where T is the sampling period, typically around tens of milliseconds, and $k = 0, 1, \ldots$. In Cartesian coordinates this translates to

$$E_{p,k}^{\mathrm{r}} = E_{p,k} \cos \varphi_{p,k}, \tag{3}$$

$$E_{p,k}^{\mathrm{i}} = E_{p,k} \sin \varphi_{p,k}. \tag{4}$$

We define the state of the power grid at time instance k as a length $2P$ real valued vector

$$\boldsymbol{s}_k = [E_{1,k}^{\mathrm{r}}, E_{1,k}^{\mathrm{i}}, E_{2,k}^{\mathrm{r}}, E_{2,k}^{\mathrm{i}}, \ldots, E_{P,k}^{\mathrm{r}}, E_{P,k}^{\mathrm{i}}]^T. \tag{5}$$

Following [7], we adopt a state space linear dynamic model

$$\boldsymbol{s}_{k+1} = \boldsymbol{A}_{1,k}\boldsymbol{s}_k + \boldsymbol{B}_{1,k}\boldsymbol{u}_{1,k} + \boldsymbol{w}_{1,k}. \tag{6}$$

The matrix $\boldsymbol{A}_{1,k}$ relates the state at the previous time step to state at current step. The matrix $\boldsymbol{B}_{1,k}$ relates the controls and other driving forces $\boldsymbol{u}_{1,k}$ to the state. The random vector $\boldsymbol{w}_{1,k}$ is assumed to be multivariate Gaussian with

$$\boldsymbol{w}_{1,k} \sim \mathcal{N}(\mathbf{0}, \boldsymbol{Q}_{1,k}). \tag{7}$$

The covariance can incorporate additional prior information, e.g., information from network topology or SCADA estimation.

The voltages on the buses are related to the currents through the branches as illustrated in Fig. 1. We denote the susceptance at bus p as B_p, and the admittance at branch $\{p, q\}$ as y_{pq}, with

$$y_{pq} = g_{pq} + j \cdot b_{pq}, \tag{8}$$

where g_{pq} is the conductance, and b_{pq} is the susceptance. These parameters are assumed to be known and constant. Consequently, the real and imaginary parts of the current on branch $\{p, q\}$ are given by

$$I_{pq,k}^{\mathrm{r}} = \left(E_{p,k}^{\mathrm{r}} - E_{q,k}^{\mathrm{r}}\right) g_{pq} - \left(E_{p,k}^{\mathrm{i}} - E_{q,k}^{\mathrm{i}}\right) b_{pq} - B_p E_{p,k}^{\mathrm{i}}, \tag{9}$$

$$I_{pq,k}^{\mathrm{i}} = \left(E_{p,k}^{\mathrm{r}} - E_{q,k}^{\mathrm{r}}\right) b_{pq} + \left(E_{p,k}^{\mathrm{i}} - E_{q,k}^{\mathrm{i}}\right) g_{pq} + B_p E_{p,k}^{\mathrm{r}}. \tag{10}$$

In an ideal setting, the power system is monitored via a network of N perfectly synchronized PMUs. For simplicity, we do not consider the use of traditional SCADA estimation. The latter may be incorporated into our model through additional prior distributions as proposed in [5]. The PMUs measure the voltages and currents located in a set of buses at time stamps kT for $k = 0, 1, \ldots$. Specifically, the PMU installed on the p'th bus measures noisy versions of

$$\tilde{\boldsymbol{z}}_k^p = \boldsymbol{H}_p \boldsymbol{s}_k^p \tag{11}$$

with

$$\begin{aligned} \tilde{\boldsymbol{z}}_k^p &= \left[E_{p,k}^{\mathrm{r}}, E_{p,k}^{\mathrm{i}}, I_{pq_1,k}^{\mathrm{r}}, I_{pq_1,k}^{\mathrm{i}}, \ldots, I_{pq_u,k}^{\mathrm{r}}, I_{pq_u,k}^{\mathrm{i}}\right]^T, \\ \boldsymbol{s}_k^p &= \left[E_{p,k}^{\mathrm{r}}, E_{p,k}^{\mathrm{i}}, E_{q_1,k}^{\mathrm{r}}, E_{q_1,k}^{\mathrm{i}}, \ldots, E_{q_u,k}^{\mathrm{r}}, E_{q_u,k}^{\mathrm{i}}\right]^T \end{aligned}$$

where $q_1, \cdots, q_u$ are the indices of the neighboring buses to bus p. The matrix $\boldsymbol{H}_p$ can be written as

$$\boldsymbol{H}_p = \begin{bmatrix} \mathbf{I} & \mathbf{0} & \cdots & \mathbf{0} \\ \boldsymbol{\Upsilon}_{pq_1} & \tilde{\boldsymbol{\Upsilon}}_{pq_1} & \cdots & \mathbf{0} \\ \vdots & \vdots & \ddots & \vdots \\ \boldsymbol{\Upsilon}_{pq_u} & \mathbf{0} & \cdots & \tilde{\boldsymbol{\Upsilon}}_{pq_u} \end{bmatrix} \tag{12}$$

where

$$\boldsymbol{\Upsilon}_{pq_i} = \begin{bmatrix} g_{pq_i} & -b_{pq_i} - B_p \\ b_{pq_i} + B_p & -b_{pq_i} \end{bmatrix} \tag{13}$$

$$\tilde{\boldsymbol{\Upsilon}}_{pq_i} = \begin{bmatrix} -g_{pq_i} & b_{pq_i} \\ -b_{pq_i} & -g_{pq_i} \end{bmatrix}. \tag{14}$$

Stacking the noisy versions of (11) for $p = 1, \cdots, N$ into one large model yields the traditional power grid observation model

$$\boldsymbol{z}_k = \tilde{\boldsymbol{z}}_k + \boldsymbol{\epsilon}_k = \boldsymbol{H}\boldsymbol{s}_k + \boldsymbol{\epsilon}_k \tag{15}$$

where $\tilde{\boldsymbol{z}}_k^p$, $\boldsymbol{H}_p$ and $\boldsymbol{s}_k^p$ are the appropriate sub-blocks of $\tilde{\boldsymbol{z}}_k$, $\boldsymbol{H}$ and $\boldsymbol{s}_k$ corresponding to the PMU on the p'th bus, and $\boldsymbol{\epsilon}_k$ is independent and identically distributed Gaussian measurement noise with $\boldsymbol{\epsilon}_k \sim \mathcal{N}(\mathbf{0}, \sigma^2\mathbf{I})$.

We now propose a more realistic state space model which takes into account the imperfect synchronization of the PMUs. The nth PMU measures its kth sample at time $kT + t_{n,k}$, where $t_{n,k}$ is a time delay. Denote the delays of all PMUs as a vector $\boldsymbol{t}_k = [t_{1,k}, \ldots, t_{N,k}]^T$. We assume that the PMUs are jointly synchronized every T_{sync} seconds. Between two synchronizations, the delays follow a linear dynamic model

$$\boldsymbol{t}_{k+1} = \boldsymbol{A}_{2,k}\boldsymbol{t}_k + \boldsymbol{B}_{2,k}\boldsymbol{u}_{2,k} + \boldsymbol{w}_{2,k}. \tag{16}$$

The control variable $\boldsymbol{u}_{2,k}$ includes temperature and other control dynamics which affect the time synchronization. The covariance of $\boldsymbol{w}_{2,k}$, $\boldsymbol{Q}_{2,k}$, can be either white Gaussian assuming independent time drifts of different sensors, or having topologically based structures associated with advanced distributed synchronization mechanisms. Recently, it has been shown in [11] that the clock state of an IEEE 1588 network satisfies a similar model.

The voltage at bus p at time instance $kT + t_{n,k}$ is

$$\begin{aligned} \overline{E}_p^c(kT + t_{n,k}) &\approx E_p^c(kT) \cos\left(2\pi f_c kT + 2\pi f_c t_{n,k} + \varphi_p^c(kT)\right) \\ &= E_{p,k} \cos\left(2\pi f_c kT + 2\pi f_c t_{n,k} + \varphi_{p,k}\right) \end{aligned}$$

where the approximation holds because $t_{n,k} \ll T$ (typically tens of microseconds in comparison to tens of milliseconds). Define the phase mismatch

$$\boldsymbol{\theta}_k = 2\pi f_{\rm c} \boldsymbol{t}_k \tag{17}$$

and use the phasor notation for the complex voltage as $E_{p,k} e^{j(\varphi_{p,k}+\theta_{p,k})}$. The real and imaginary parts of this delayed voltage can be expressed as

$$\tilde{E}^{\rm r}_{p,k} = E_{p,k} \cos(\varphi_{p_k} + \theta_{p,k}) \approx E^{\rm r}_{p,k} - E^{\rm i}_{p,k}\theta_{p,k}, \tag{18}$$

$$\tilde{E}^{\rm i}_{p,k} = E_{p,k} \sin(\varphi_{p_k} + \theta_{p,k}) \approx E^{\rm i}_{p,k} - E^{\rm r}_{p,k}\theta_{p,k}, \tag{19}$$

where we have used the standard approximation

$$\sin\theta_{p,k} \approx \theta_{p,k}, \quad \cos\theta_{p,k} \approx 1, \tag{20}$$

which holds for small values of θ_p (typically, less than 1 degree corresponding to 46.3 μs delay at $f_{\rm c} = 60$Hz). The delayed currents are provided in (21) and (22) below, where the subscript k is omitted for brevity. Note that all the measurements from the PMU installed on a particular bus, namely the voltage and the currents on all the adjacent branches, are associated with the same phase mismatch θ_p, as they use the same time stamp. Thus, the imperfectly synchronized version of (11) is given by

$$\tilde{\boldsymbol{z}}^p_k = \boldsymbol{H}_p \boldsymbol{s}^p_k + \theta_{p,k} \boldsymbol{G}_p \boldsymbol{s}^p_k \tag{23}$$

where $\boldsymbol{H}_p$ is defined in (12) and $\boldsymbol{G}_p$ is

$$\boldsymbol{G}_p = \begin{bmatrix} -\tilde{\mathbf{I}} & \mathbf{0} & \cdots & \mathbf{0} \\ \boldsymbol{\Xi}_{pq_1} & \tilde{\boldsymbol{\Xi}}_{pq_1} & \cdots & \mathbf{0} \\ \vdots & \vdots & \ddots & \vdots \\ \boldsymbol{\Xi}_{pq_u} & \mathbf{0} & \cdots & \tilde{\boldsymbol{\Xi}}_{pq_u} \end{bmatrix} \tag{24}$$

where

$$\tilde{\mathbf{I}} = \begin{bmatrix} 0 & 1 \\ 1 & 0 \end{bmatrix} \tag{25}$$

$$\boldsymbol{\Xi}_{pq_i} = \begin{bmatrix} b_{pq_i} + B_p & -g_{pq_i} \\ -g_{pq_i} & -b_{pq_i} - B_p \end{bmatrix} \tag{26}$$

$$\tilde{\boldsymbol{\Xi}}_{pq_i} = \begin{bmatrix} -b_{pq_i} & g_{pq_i} \\ g_{pq_i} & b_{pq_i} \end{bmatrix}. \tag{27}$$

Stacking these observations together with additive noise yields the following bilinear observation model

$$\boldsymbol{z}_k = \left(\boldsymbol{H} + \sum_{n=1}^{N} \theta_{n,k} \boldsymbol{G}_n \right) \boldsymbol{s}_k + \boldsymbol{\epsilon}_k \tag{28}$$

where $\boldsymbol{\epsilon}_k$ is i.i.d. Gaussian measurement noise following $\mathcal{N}(\mathbf{0}, \sigma^2\mathbf{I})$.

III. State Estimation Considering Phase Mismatch

In the previous section we formulated the power grid statistical models. In the classical setting defined in (6) and (15), state estimation is the problem of recovering $\boldsymbol{s}_k$ given $\boldsymbol{z}_k, \boldsymbol{z}_{k-1}, \cdots, \boldsymbol{z}_0$. It is traditionally solved using Kalman filtering [15], [19]-[21]. In this work, we proposed a more realistic model defined in (6), (16) and (28). This formulation involves additional nuisance parameters $\boldsymbol{t}_k$ which complicate the inference of $\boldsymbol{s}_k$. The optimal filter solution requires the computation of the posterior distribution of unknown state parameters marginalized over the nuisance parameters, and is clearly intractable. Instead, we propose an approximate solution based on joint estimation of both $\boldsymbol{s}_k$ and $\boldsymbol{t}_k$ via two parallel yet coupled Kalman filters. We also propose a simple static estimation approach which is competitive with dynamic filtering under some settings.

A. Static State Estimation

Static state estimation considers the estimation of $\boldsymbol{s}_k$ given $\boldsymbol{z}_k$. It does not assume the dynamical models in (6) and (16). Instead of the dynamic characterization, we propose simple Gaussian priors on the time delays

$$\boldsymbol{t}_k \sim \mathcal{N}(\mathbf{0}, \sigma_t^2\mathbf{I}), \tag{29}$$

and as a result the phase mismatches $\boldsymbol{\theta}$ follow a similar Gaussian prior $\mathcal{N}(\mathbf{0}, \sigma_\theta^2\mathbf{I})$. For simplicity and robustness, we model the state as a deterministic unknown vector. Additional information can be easily incorporated by an additional state prior.

The optimal solution to static state estimation with nuisance parameters is computationally intensive. Instead, we propose an approximate technique that jointly estimates both unknowns. Due to the bilinear structure of (28), the solution for each of these parameters assuming the other is known has a simple closed form . Thus, we propose the following alternating algorithm, where $\boldsymbol{\Psi}_k = \boldsymbol{\Psi}(\boldsymbol{s}_k)$ and $\boldsymbol{\Phi}_k = \boldsymbol{\Phi}(\boldsymbol{\theta}_k)$, and $\lambda = \sigma^2/\sigma_\theta^2$. More details of this algorithm can be found in [22].

Data: observations $\boldsymbol{z}_k$.
Result: state estimation $\boldsymbol{s}_k$.
begin
  $\boldsymbol{\theta}_k = \mathbf{0}$;
  repeat
    $\boldsymbol{s}_k \leftarrow (\boldsymbol{\Phi}_k^T\boldsymbol{\Phi}_k)^{-1}\boldsymbol{\Phi}_k^T\boldsymbol{z}_k$;
    $\boldsymbol{\theta}_k \leftarrow (\boldsymbol{\Psi}_k^T\boldsymbol{\Psi}_k + \lambda\mathbf{I})^{-1}\boldsymbol{\Psi}_k^T(\boldsymbol{z}_k - \boldsymbol{H}\boldsymbol{s}_k)$;
  until *convergence or max iterations achieved*;
end

Algorithm 1: Alternating approach for static estimation.

The main disadvantage of Algorithm 1 is that multiple iterations have to be executed at each sample. However, under the assumption that the phase mismatch changes slowly, the phase mismatch from a previous time point $\boldsymbol{\theta}_{k-1}$ can be used to "warm start" the estimation of the next time point $\boldsymbol{\theta}_k$, thus reducing the number of iterations.

B. Dynamic State Estimation

In this subsection, we consider a dynamic filtering solution for the case in which the phase mismatch significantly changes over time. The system state $\boldsymbol{s}_k$ and time delays $\boldsymbol{t}_k$ follow the previously defined linear dynamic models (6) and (16), where in (16) the time $\boldsymbol{t}_k$ is substituted by phase $\boldsymbol{\theta}_k$. The

$$\begin{aligned}\tilde{I}^{\mathrm{r}}_{pq} =& \left(E_p\cos(\varphi_p+\theta_p)-E_q\cos(\varphi_q+\theta_p)\right)g_{pq}-\left(E_p\sin(\varphi_p+\theta_p)-E_q\sin(\varphi_q+\theta_p)\right)b_{pq}-B_pE_p\sin(\varphi_p+\theta_p)\\ \approx& E^{\mathrm{r}}_p\left(g_{pq}+b_{pq}\theta_p+B_p\theta_p\right)+E^{\mathrm{r}}_q\left(-g_{pq}-b_{pq}\theta_p\right)+E^{\mathrm{i}}_p\left(-g_{pq}\theta_p-b_{pq}-B_p\right)+E^{\mathrm{i}}_q\left(g_{pq}\theta_p+b_{pq}\right),\end{aligned} \tag{21}$$

$$\begin{aligned}\tilde{I}^{\mathrm{i}}_{pq} =& \left(E_{p,k}\cos(\varphi_p+\theta_p)-E_q\cos(\varphi_q+\theta_p)\right)b_{pq}+\left(E_p\sin(\varphi_p+\theta_p)-E_q\sin(\varphi_q+\theta_p)\right)g_{pq}+B_pE_p\cos(\varphi_p+\theta_p)\\ \approx& E^{\mathrm{r}}_p\left(b_{pq}-g_{pq}\theta_p+B_p\right)+E^{\mathrm{r}}_q\left(-b_{pq}+g_{pq}\theta_p\right)+E^{\mathrm{i}}_p\left(-b_{pq}\theta_p+g_{pq}-B_p\theta_p\right)+E^{\mathrm{i}}_q\left(b_{pq}\theta_p-g_{pq}\right).\end{aligned} \tag{22}$$

measurement model at time instance k based on (28) can be written as

$$\boldsymbol{z}_k = \boldsymbol{H}\boldsymbol{s}_k + \left(\sum_{n=1}^{N}\boldsymbol{\theta}_{n,k}\boldsymbol{G}_{n,k}\right)\boldsymbol{s}_k + \boldsymbol{\epsilon}_k, \tag{30}$$

where $\boldsymbol{\epsilon}_k \sim \mathcal{N}(\mathbf{0}, \boldsymbol{R}_k)$. We add a subscript k to matrices $\boldsymbol{G}_n$, because in this dynamic system, the system topology or parameters might change over time. Let

$$\boldsymbol{C}_1(\boldsymbol{\theta}_k) = \sum_{n=1}^{N}\theta_{n,k}\boldsymbol{G}_{n,k}, \tag{31}$$

$$\boldsymbol{C}_2(\boldsymbol{s}_k) = [\boldsymbol{G}_{1,k}\boldsymbol{s}_k, \boldsymbol{G}_{2,k}\boldsymbol{s}_k, \cdots, \boldsymbol{G}_{N,k}\boldsymbol{s}_k]. \tag{32}$$

(30) can be rewritten as

$$\boldsymbol{z}_k = \boldsymbol{H}\boldsymbol{s}_k + \boldsymbol{C}_1(\boldsymbol{\theta}_k)\boldsymbol{s}_k + \boldsymbol{\epsilon}_k, \tag{33}$$

$$\boldsymbol{z}_k = \boldsymbol{H}\boldsymbol{s}_k + \boldsymbol{C}_2(\boldsymbol{s}_k)\boldsymbol{\theta}_k + \boldsymbol{\epsilon}_k. \tag{34}$$

We propose to solve this model using PKF [18]. We couple two Kalman filters, one for state estimation and one for phase mismatch estimation. When observation $\boldsymbol{z}_k$ is received, we first estimate the phase mismatch $\boldsymbol{\theta}_k$, and then estimate the system state $\boldsymbol{s}_k$. The formulas for estimating the state and phase mismatch are listed below.

- State estimation

$$\begin{aligned}\hat{\boldsymbol{s}}_{k|k-1} &= \boldsymbol{A}_{1,k}\hat{\boldsymbol{s}}_{k-1|k-1} + \boldsymbol{B}_{1,k}\boldsymbol{u}_k\\ \boldsymbol{P}^{(s)}_{k|k-1} &= \boldsymbol{A}_{1,k}\boldsymbol{P}^{(s)}_{k-1|k-1}\boldsymbol{A}^T_{1,k} + \boldsymbol{Q}_{1,k}\\ \boldsymbol{K}^{(s)}_k &= \boldsymbol{P}^{(s)}_{k|k-1}\left(\boldsymbol{H}+\boldsymbol{C}_1(\boldsymbol{\theta}_{k|k-1})\right)^T\\ &\quad\left(\left(\boldsymbol{H}+\boldsymbol{C}_1(\boldsymbol{\theta}_{k|k-1})\right)\boldsymbol{P}^{(s)}_{k|k-1}\left(\boldsymbol{H}+\boldsymbol{C}_1(\boldsymbol{\theta}_{k|k-1})\right)^T + \boldsymbol{R}_k\right)^{-1}\\ \boldsymbol{P}^{(s)}_{k|k} &= \boldsymbol{P}^{(s)}_{k|k-1} - \boldsymbol{K}^{(s)}_k\left(\boldsymbol{H}+\boldsymbol{C}_1(\boldsymbol{\theta}_{k|k-1})\right)\boldsymbol{P}^{(s)}_{k|k-1}\\ \hat{\boldsymbol{s}}_{k|k} &= \hat{\boldsymbol{s}}_{k|k-1} + \boldsymbol{K}^{(s)}_k\left(\boldsymbol{z}_k - \left(\boldsymbol{H}+\boldsymbol{C}_1(\boldsymbol{\theta}_{k|k-1})\right)\hat{\boldsymbol{s}}_{k|k-1}\right).\end{aligned}$$

- Phase mismatch estimation

$$\begin{aligned}\hat{\boldsymbol{\theta}}_{k|k-1} &= \boldsymbol{A}_{2,k}\hat{\boldsymbol{\theta}}_{k-1|k-1} + \boldsymbol{B}_{2,k}\boldsymbol{u}_k\\ \boldsymbol{P}^{(\theta)}_{k|k-1} &= \boldsymbol{A}_{2,k}\boldsymbol{P}^{(\theta)}_{k-1|k-1}\boldsymbol{A}^T_{2,k} + \boldsymbol{Q}_{2,k}\\ \boldsymbol{K}^{(\theta)}_k &= \boldsymbol{P}^{(\theta)}_{k|k-1}\boldsymbol{C}_2(\boldsymbol{s}_{k|k-1})^T\\ &\quad\left(\boldsymbol{C}_2(\boldsymbol{s}_{k|k-1})\boldsymbol{P}^{(s)}_{k|k-1}\boldsymbol{C}_2(\boldsymbol{s}_{k|k-1})^T + \boldsymbol{R}_k\right)^{-1}\\ \boldsymbol{P}^{(s)}_{k|k} &= \boldsymbol{P}^{(s)}_{k|k-1} - \boldsymbol{K}^{(s)}_k\boldsymbol{C}_2(\boldsymbol{s}_{k|k-1})\boldsymbol{P}^{(\theta)}_{k|k-1}\\ \hat{\boldsymbol{\theta}}_{k|k} &= \hat{\boldsymbol{\theta}}_{k|k-1} + \boldsymbol{K}^{(\theta)}_k\left(\boldsymbol{z}_k - \left(\boldsymbol{H}\hat{\boldsymbol{s}}_{k|k-1} + \boldsymbol{C}_2(\boldsymbol{s}_{k|k-1})\boldsymbol{\theta}_k\right)\right).\end{aligned}$$

Our filters exploit the fact that the PMUs are synchronized every few seconds. For this purpose, we reset the phase filter at time of synchronization as discussed in [22].

IV. Numerical Examples

A. General Setup

We assume the PMUs sample at a rate of $30\ \mathrm{samples/s}$, and are synchronized every 2 seconds (60 samples). Namely, the phase mismatches change every 2 seconds, and are assumed to be unchanging within a 2-second interval. For the static estimation case, we select $\sigma_t = 25\mu$s and $\sigma = 5\times10^{-3}$ p.u. For the dynamic case, we generate $\boldsymbol{t}_k$ using (16) with $\boldsymbol{Q}_{2,k} = \sigma_d^2\boldsymbol{I}$ and $\sigma_d = 5\ \mu$s. We use the root mean squared error (RMSE) as the performance measure. For each time point, we calculate the RMSE of the magnitude and angle of the bus voltages, and then average the RMSE over all the time points. In each test we execute 20 Monte-Carlo simulations with 600 data points (equivalent to 20 seconds of data), and the system states are generated using (6), with $\boldsymbol{Q}_{1,k} = \sigma_s^2\mathbf{I}$. We select $\sigma_s = 10^{-3}$ p.u. as the change of states is relatively slow comparing with the high sample rate. The initial magnitude $\boldsymbol{E}_0$ and angle $\boldsymbol{\varphi}_0$ for each Monte-Carlo simulation are generated from the following distributions

$$\begin{aligned}\boldsymbol{E}_0 &\sim \mathcal{N}(\mathbf{1}, 0.05^2\mathbf{I}) \quad \text{p.u.},\\ \boldsymbol{\varphi}_0 &\sim \mathcal{U}(\mathbf{0}, \boldsymbol{2\pi}) \quad \text{rad.}\end{aligned} \tag{35}$$

For each test system, we consider two scenarios - one with the minimum number of PMUs installed for full (topological) observation, and one with redundant observations on selected buses. In this numerical example, the buses with redundant observations are randomly selected. In reality, we can assign more redundant observations on pre-specified important buses.

B. Estimation Results

1) Static estimation results: Under the general setup, we run Algorithm 1 for static state estimation. The state and phase mismatch error at one time point are shown in Fig. 2. Note that we convert the real-imaginary representation into magnitudes and angles for easier comparison. When considering phase mismatch in the estimation model, and employing the AM algorithm for state estimation, we observe that the estimation errors in both magnitude and angle are reduced.

We show the RMSE on other systems in Table I, where we include the "Oracle" case for comparison. The oracle estimation is obtained by assuming perfect knowledge of the phase mismatch. We observe that on all the tested systems, the AM provides more accurate estimates than the LS. As expected, the improvement is more significant when there are redundant observations, as the redundant observation will provide more measurements. We also observe that when the number of PMUs increase, the AM estimation is closer to the oracle case.

TABLE I: Root mean-squared error of static estimation on different test systems using least-squares estimation (LS), alternating minimization (AM), and LS with perfect phase mismatch information (Oracle).

# of Buses	# of PMUs	Least Squares Magnitude (p.u.)	Least Squares Angle (degrees)	Alternating Minimization Magnitude (p.u.)	Alternating Minimization Angle (degrees)	Oracle Magnitude (p.u.)	Oracle Angle (degrees)	$\mathrm{RMSE_{AM}}/\mathrm{RMSE_{LS}}$ Magnitude (ratio)	$\mathrm{RMSE_{AM}}/\mathrm{RMSE_{LS}}$ Angle (ratio)
14	4	6.400e-03	0.3973	3.746e-03	0.2302	1.443e-03	0.0834	58.52%	57.95%
	6	6.812e-03	0.3348	2.681e-03	0.1578	1.017e-03	0.0587	39.36%	47.14%
30	10	5.232e-03	0.3463	4.739e-03	0.2865	2.994e-03	0.1719	90.57%	82.74%
	16	3.527e-03	0.2797	2.387e-03	0.1540	1.630e-03	0.0944	67.67%	55.05%
57	17	6.639e-03	0.4101	6.389e-03	0.3778	4.227e-03	0.2426	96.24%	92.14%
	28	4.955e-03	0.3260	2.153e-03	0.1390	1.448e-03	0.0832	43.45%	42.63%
118	32	8.678e-03	0.5417	4.285e-03	0.2545	2.219e-03	0.1281	49.38%	46.98%
	54	7.218e-03	0.4894	2.078e-03	0.1290	0.727e-03	0.0419	28.79%	26.36%

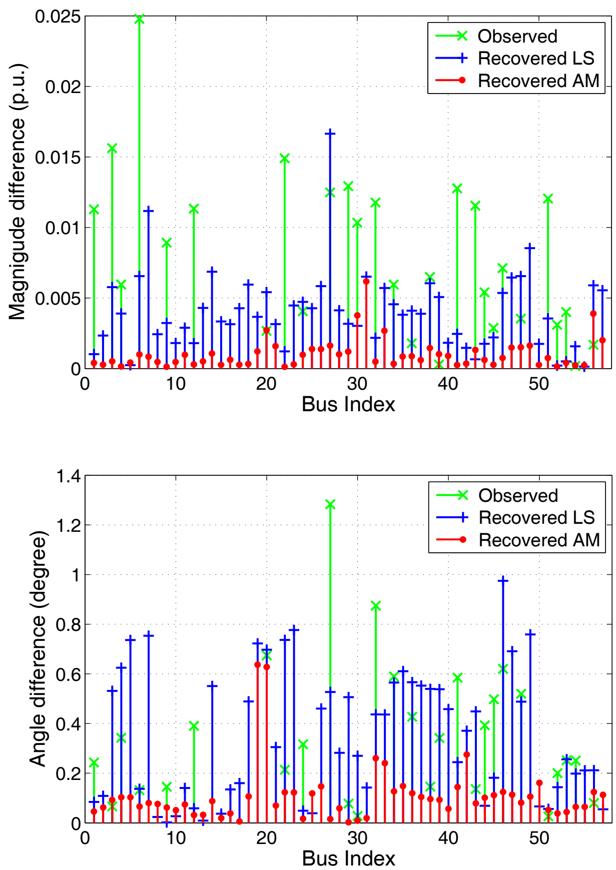

Fig. 2: Static estimation using alternating minimization algorithm on the IEEE 57-Bus system with 28 PMUs at $t = 8$ s.

2) Dynamic estimation example: We compare the proposed PKF which estimates the phase mismatch, with the traditional Kalman filter (KF) which ignores the phase mismatch. We show the RMSE at each time instance of 8 seconds in Fig. 3, where the vertical dotted line denotes the time of synchronization. The figures indicate that by using PKF, we can accurately estimate the phase mismatch, and the estimation accuracy of system state is significantly increased. Table II shows the improvement of estimation accuracy on different test systems.

TABLE II: Root mean-squared error of dynamic estimation on different test systems using traditional and parallel Kalman filter.

# of Buses	# of PMUs	Kalman Filter Magnitude (p.u.)	Kalman Filter Angle (degrees)	Parallel Kalman Filter Magnitude (p.u.)	Parallel Kalman Filter Angle (degrees)
14	4	6.449e-03	0.3458	3.596e-03	0.1894
	6	6.258e-03	0.3293	3.242e-03	0.1766
30	10	4.249e-03	0.2852	3.026e-03	0.1901
	16	3.311e-03	0.2600	2.169e-03	0.1549
57	17	5.096e-03	0.3301	4.165e-03	0.2616
	28	4.415e-03	0.3237	2.169e-03	0.1616
118	32	8.720e-03	0.5933	4.243e-03	0.2564
	54	7.599e-03	0.5225	3.797e-03	0.2604

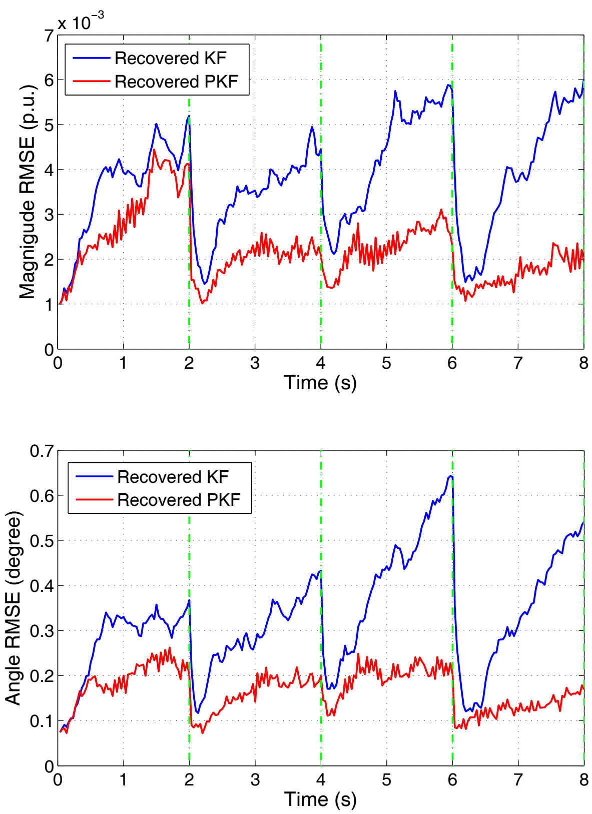

Fig. 3: Dynamic estimation results on IEEE 57-bus system with 28 PMUs from $t = 0$ s to $t = 8$ s.

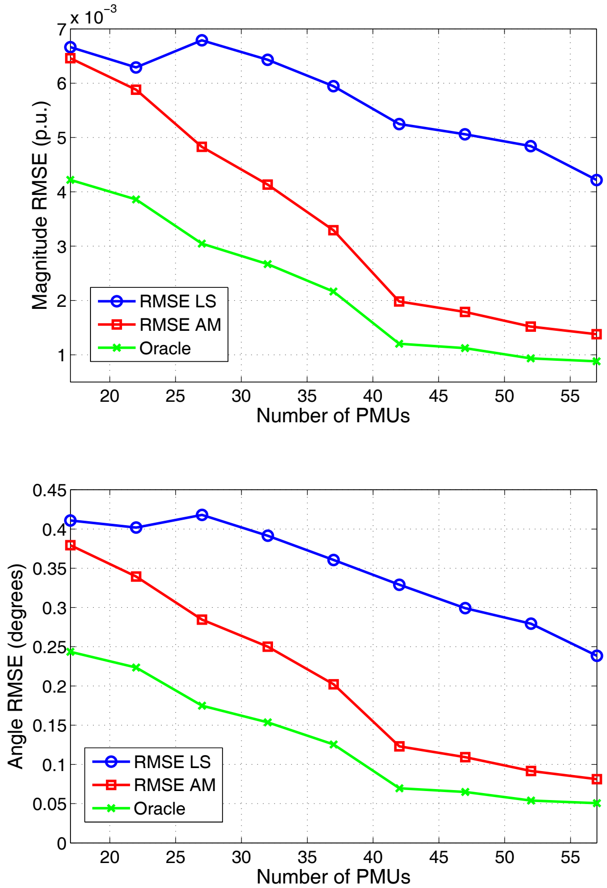

Fig. 4: RMSE as a function of number of PMUs installed on IEEE 57-bus system with $\sigma_t = 25\mu$s .

C. Effect of Number of PMUs

The number of installed PMUs affect the estimation performance. In Fig. 4 we plot the estimation error as a function of the number of PMUs installed when σ_t is fixed and constant for all PMUs. We observe that the performance improves as more PMUs are installed. As expected, this improvement is more significant when more PMUs are installed, in which case the performance gap to the oracle also decreases.

V. Conclusion

In this paper, we considered models and estimation techniques for static and dynamic power state estimation using PMUs with imperfect synchronization. We demonstrated that when a sufficient number of PMUs are employed, the phase mismatch can be largely compensated by signal processing methods under our proposed model. This conclusion encourages large scale deployment of imperfectly synchronized but low cost PMUs. In future work, we will derive analytical performance bounds for our algorithms, and consider optimal PMU placement problems based on our realistic statistical model.

Acknowledgement

The authors would like to thank Prof. Danny Dolev and Dr. Tal Anker for introducing us to IEEE-1588.

Ami Wiesel was supported by the Israel Smart Grid (ISG) consortium.

References

[1] J. De La Ree, V. Centeno, J. Thorp, and A. Phadke, "Synchronized phasor measurement applications in power systems," *IEEE Trans. Smart Grid*, vol. 1, no. 1, pp. 20 –27, Jun. 2010.

[2] F. Schweppe and E. Handschin, "Static state estimation in electric power systems," *Proc. IEEE*, vol. 62, no. 7, pp. 972–982, Aug. 1974.

[3] A. Monticelli, *State Estimation in Electric Power Systems: a Generalized Approach*. New York: Springer, 1999.

[4] A. Abur and A. G. Expósito, *Power System State Estimation: Theory and Implementation*. New York: Marcel Dekker, Inc., 2004.

[5] V. Kekatos, G. B. Giannakis, and B. Wollenberg, "Optimal placement of phasor measurement units via convex relaxation," *IEEE Trans. Power Syst.*, vol. 27, no. 3, pp. 1521 –1530, Aug. 2012.

[6] B. Gou, "Generalized integer linear programming formulation for optimal PMU placement," *IEEE Trans. Power Syst.*, vol. 23, no. 3, pp. 1099 –1104, aug. 2008.

[7] J. Zhang, G. Welch, and G. Bishop, "Observability and estimation uncertainty analysis for PMU placement alternatives," in *North American Power Symposium (NAPS), 2010*, Sep. 2010, pp. 1–8.

[8] KEMA, Inc., "Substation communications: Enabler of automation / an assessment of communications technologies," United Telecom Council, Tech. Rep., Nov. 2006.

[9] A. P. Meliopoulos, V. Madani, and D. N. *et. al*, "Synchrophasor measurement accuracy characterization," North American SynchroPhasor Initiative Performance & Standards Task Team, Tech. Rep., Aug. 2007.

[10] C. Na, D. Obradovic, and R. Scheiterer, "A probabilistic approach to clock synchronization of cascaded network elements," in *ICASSP 2009*, Apr. 2009, pp. 1793–1796.

[11] G. Giorgi and C. Narduzzi, "Performance analysis of Kalman-filter-based clock synchronization in IEEE 1588 networks," *IEEE Trans. Instrum. Meas.*, vol. 60, no. 8, pp. 2902–2909, Aug. 2011.

[12] M. Kezunovic, A. Sprintson, J. Ren, and Y. Guan, "Signal processing, communication, and networking requirements for synchrophasor systems," in *13th International Workshop on Signal Processing Advances in Wireless Communications (SPAWC)*, Jun. 2012, pp. 464 –468.

[13] P. Top, M. Bell, E. Coyle, and O. Wasynczuk, "Observing the power grid: Working toward a more intelligent, efficient, and reliable smart grid with increasing user visibility," *IEEE Signal Process. Mag.*, vol. 29, no. 5, pp. 24 –32, Sep. 2012.

[14] M. Zhou, V. Centeno, J. Thorp, and A. Phadke, "An alternative for including phasor measurements in state estimators," *IEEE Trans. Power Syst.*, vol. 21, no. 4, pp. 1930 –1937, Nov. 2006.

[15] A. Jain and N. Shivakumar, "Impact of PMU in dynamic state estimation of power systems," in *40th North American Power Symposium*, Sep. 2008, pp. 1–8.

[16] E. Farantatos, G. Stefopoulos, G. Cokkinides, and A. Meliopoulos, "PMU-based dynamic state estimation for electric power systems," in *Power Energy Society General Meeting*, Jul. 2009, pp. 1–8.

[17] V. Kekatos and G. B. Giannakis, "Distributed robust power system state estimation," *arXiv:1204.0991v2*, Apr. 2012.

[18] L. Glielmo, P. Marino, R. Setola, and F. Vasca, "Parallel Kalman filter algorithm for state estimation in bilinear systems," in *33rd Conference on Decision and Control*, Dec. 1994, pp. 1228–1229.

[19] H. Beides and G. Heydt, "Dynamic state estimation of power system harmonics using Kalman filter methodology," *IEEE Trans. Power Del.*, vol. 6, no. 4, pp. 1663 –1670, Oct. 1991.

[20] K.-R. Shih and S.-J. Huang, "Application of a robust algorithm for dynamic state estimation of a power system," *IEEE Trans. Power Syst.*, vol. 17, no. 1, pp. 141–147, Feb. 2002.

[21] G. Valverde and V. Terzija, "Unscented kalman filter for power system dynamic state estimation," *IET Generation, Transmission Distribution*, vol. 5, no. 1, pp. 29 –37, Jan. 2011.

[22] P. Yang, Z. Tan, A. Wiesel, and A. Nehorai, "Power system state estimation using PMUs with imperfect synchronization," *submitted to IEEE Trans. Power Syst.*